Available online at www.sciencedirect.com
ScienceDirect
International Journal of Pharmaceutics 343 (2007) 131–140
INTERNATIONAL JOURNAL OF PHARMACEUTICS
www.elsevier.com/locate/ijpharm

Vitrification from solution in restricted space: Formation and stabilization of amorphous nifedipine in a nanoporous silica xerogel carrier

Aljaž Godec [a,b], Uroš Maver [a,b], Marjan Bele [a], Odon Planinšek [b], Stane Srčič [b], Miran Gaberšček [a,*], Janko Jamnik [a]

[a] National Institute of Chemistry, Hajdrihova 19, 1000 Ljubljana, Slovenia
[b] Faculty of Pharmacy, University of Ljubljana, Aškerčeva 7m, 1000 Ljubljana, Slovenia

Received 20 November 2006; received in revised form 26 April 2007; accepted 9 May 2007
Available online 18 May 2007

Abstract

Purpose: The goal was to find thermodynamic criteria that must be satisfied in order to prevent formation of crystalline state of drugs within a confined space (e.g., nanopores of inorganic solid). Similarly, criteria that lead to stabilization of amorphous drug within such pores were investigated.
Methods: In the theoretical part, the classical thermodynamics of nucleation is applied to the conditions of a restricted space. The theoretical findings are verified using porous silica as a carrier and nifedipine as a model drug. The amorphicity of the latter is checked using XRD and thermal analysis (DTA, DSC) in combination with BET measurements.
Results: It is shown that there exists a critical pore radius of a host below which the entrapped substance will solidify in an amorphous form. There also exists a critical pore radius below which the entrapped amorphous solid will not be able to crystallize. Specifically, incorporation of NIF into a silica xerogel with an average pore diameter of about 2.5 nm produces and stabilizes its amorphous form.
Conclusion: Entrapment of drugs into solid nanoporous carriers could be regarded as a potentially useful and simple method for production and/or stabilization of non-crystalline forms of a wide range of drugs.

Keywords: Thermodynamics; Nucleation; Amorphous drugs; Structural stabilization; Porous carriers

1. Introduction

Incorporation of solid substances into appropriate porous matrices has been a subject of numerous investigations (Böhlmann et al., 1999; Lucas et al., 2001; Czuryszkiewicz et al., 2002; Quaranta et al., 2003; Maria Chong and Zhao, 2004; Vallet-Regi et al., 2004; Chytil et al., 2005; Zhao et al., 2005; Prasad and Quijano, 2006). In the case of drug incorporation, for example, the common goal has been control of drug release. It is reasonable to expect that the average rate of drug release will be decreased if a drug is entrapped into a web of pores within a solid inorganic host material. With emerging nanosciences and nanotechnologies, entrapment into "nanosized pores" (conventionally termed meso- or micropores, if size <50 nm or <2 nm, respectively) has become particularly popular. The thorough research in this area has resulted in many interesting findings shedding light on the nature of matter confined in nano-domains of host material (Shin and Chang, 2001; Chong and Zhao, 2004; Kim et al., 2004; Bögershausen et al., 2007; Sotiropoulou and Vamvakaki, 2005; Kim et al., 2006; Wang and Song, 2006). However, in all these studies the authors apparently neglected a very important phenomenon that is expected to occur when matter is confined into a small space – the possible change of its structure. Namely, it is known from the classical nucleation-and-growth theory (Defay, 1966; Adamson and Gast, 1997; Sugimoto, 2001; Christian, 2002) that typical nuclei formed in the course of crystallization process consist of many (tens to hundreds) constituent particles (atoms, molecules). If so, several fundamental questions *par excellence* arise: What happens if there is not enough space for nuclei to form? Does matter confined into nanosized pores inherently solidify in the amor-

* Corresponding author at: National Institute of Chemistry Slovenia, Hajdrihova 19, SI-1000 Ljubljana, Slovenia. Tel.: +386 1 4760 320; fax: +386 1 4760 300.
E-mail address: miran.gaberscek@ki.si (M. Gaberšček).

0378-5173/$ – see front matter © 2007 Elsevier B.V. All rights reserved.
doi:10.1016/j.ijpharm.2007.05.022

phous rather than in the crystalline state and, if yes, what are the critical pore dimensions when the transition from one to the other state occurs? And finally: What is the stability of the amorphous state within the confined space (e.g., within pores, channels) of host matrix? We try to answer these fundamental questions both theoretically and experimentally, using an example of pharmaceutical interest, that is, entrapment of nifedipine into silica nanosized pores. The treatment itself, however, is general enough that the findings can be generalized to most solid materials confined within restricted domains of host materials.

In the theoretical part, we refer to the classical theory of nucleation based on random fluctuations in a metastable assembly. This theory was mainly developed by Volmer, Becker and Döring (Volmer, 1939), although other workers have also made significant contributions. It was first formulated for the simplest nucleation process, the condensation of a pure vapour to form a liquid. Later on, it was modified to describe systems such as nucleation in solution, in a supercooled melt, in the solid state (Christian, 2002). The formation of a stable nucleus in contact with a surface (heterogenous nucleation) was introduced by Volmer (Volmer, 1929). Turnbull expanded the treatment to the nucleation process in cylindrical and conical cavities (Turnbull, 1950a). Massive research has been done in the field of nucleation in the vitreous state (Rowlands and James, 1979a,b; Shneidman and Weinberg, 1996; Wakayama et al., 1999; Andronis and Zografi, 2000). A theory for the nucleation in solid solutions has also been developed (Slezov et al., 1997). Recently, the influence of elastic strain on the thermodynamics and kinetics of nucleation in the vitreous state was studied by Gutzow and Schmelzer (Schmelzer et al., 1995; Möller et al., 1998; Schmelzer et al., 2004; Fokin et al., 2005).

Based on these and similar works, we formulate general thermodynamic criteria that must be satisfied for occurrence of crystalline matter from saturated solution confined within a restricted space. We further formulate similar general criteria for formation of confined amorphous solid matter. The occurrence of amorphous phase upon cooling of the melt in pores below a certain pore size has been reported in the case *o*-terphenyl, benzyl alcohol (Jackson and McKenna, 1996) and nitrobenzene (Sliwinska-Bartkowiak et al., 2001) confined into nanoporous glass materials.

In the experimental part, the validity of the theoretically developed criteria for crystallization from supersaturated solution and from amorphous state, respectively, is checked. As a model system, we selected nifedipine (NIF) entrapped in a porous silica xerogel. NIF, a potent systemic calcium channel blocker, was chosen because of its high crystallinity, poor solubility in water and a high tendency of its amorphous form to crystallize. It is used in the treatment of angina pectoris and hypertension. Silica xerogels are well-known carrier systems exhibiting significant porosity on the nanometre scale. Zusman et al. (1990) reported the use of doped silica glasses for pH sensors in analytical chemistry. Chen and Dong (2003) and Shankaran et al. (2003) produced sol–gel composite based glucose biosensors. Conventional drug molecules have also been incorporated into silica xerogels, mostly to achieve controlled release. Kortesuo and Ahola (2001, 2002) studied the effect of synthesis parameters on the release rate of dexmedetomidine from silica gel microparticles and monoliths. Ahola and Kortesuo (2000) produced silica xerogel carrier material for controlled release of teoremifene citrate. Tian and Blacher (1999) studied the effect of acid and water content on the incorporation of aliphatic polyesters into silica gels.

2. Theoretical

2.1. Crystallization from supersaturated solution in restricted space

It is well-known that the process of crystallization consists of two steps: formation of nuclei (that is, clusters of atoms, molecules, etc.) and their subsequent growth (Defay, 1966; Adamson and Gast, 1997; Sugimoto, 2001; Christian, 2002). The formation of critical nuclei may be viewed as random fluctuations of density, in which about 50–250 molecules come together to form a nucleus of the size observed experimentally (Defay, 1966). Based on this fundamental knowledge, we hypothesize that entrapment of a dissolved drug into a solid matrix that contains constrained spaces (e.g., pores) smaller than the critical nucleation radius, will prevent the process of drug crystallization upon removal of solvent. The resulting solid drug is then expected to occur in the amorphous rather than in crystalline form.

We assume that all pores in a given solid matrix (for example, porous silica carrier) are of the same shape and size with no preferential sites on the surface. Let the pores contain a saturated solution of a drug. There are two possible sites for nucleation to start: either on the existing solid surfaces (walls of silica pores) or in the volume of saturated solution. The former scenario (heterogeneous nucleation) will take place if the contact angle between the embryo of the new solid phase and the surface of the existing phase, θ (Fig. 1) is within the range $0 \leq \theta \leq \pi$ (Christian, 2002). Then the following equation will hold:

$$\gamma^{AS} = \gamma^{BS} - \gamma^{AB} \cos\theta \quad (1)$$

where γ^{XY} is the interfacial free energy between phases X and Y. If, however, θ is outside the aforementioned limits, the phase with the lower interfacial energy spreads over the whole solid surface and Eq. (1) does not hold anymore. In this case, nucleation in the bulk solution (homogeneous nucleation) is expected to occur—*pure confinement effect*. To determine which of the

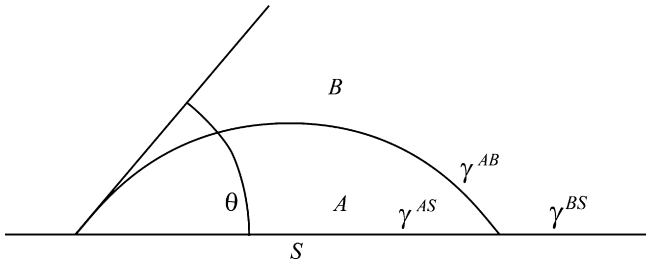

Fig. 1. Hypothetical embryo formed on a solid surface. In the present context, B could represent the NIF solution, S the silica surface, and A a crystalline nucleus of NIF.

two scenarios will take place in a given system, one can estimate the interfacial free energies γ^{XY} using the following equation: (Wu, 1971)

$$\gamma^{XY} = \gamma_X + \gamma_Y - 2\sigma^d - 2\sigma^p \equiv \gamma_X + \gamma_Y - \frac{4\gamma_X^D\gamma_Y^D}{\gamma_X^D + \gamma_Y^D} - \frac{4\gamma_X^P\gamma_Y^P}{\gamma_X^P + \gamma_Y^P}, \quad (2)$$

where γ_X and γ_Y are surface free energies of phases X and Y, the terms σ^p and σ^d reflect specific and dispersive interactions between X and Y, γ_X^D and γ_Y^D are dispersive components and γ_X^P and γ_X^P are specific components of surface free energies of X and Y. Eq. (2) indicates that the interfacial free energies will be the lower, the more similar are the polarities of phases X and Y.

As shown in Section 4, Eqs. (1) and (2) predict that homogeneous nucleation of nifedipine in bulk solution within silica pores is more likely than heterogeneous nucleation of the drug on the walls of pores. According to the classical nucleation theory (Adamson and Gast, 1997; Sugimoto, 2001; Christian, 2002), the free energy of formation of a nucleus in the bulk solution, $W^{solution}$, is obtained as follows:

$$W^{solution} = -n\phi + \sum_i A_i\bar{\gamma} \equiv -nkT\ln S + \left(\frac{\nu_1 k_2^{3/2}}{k_3}\right)^{2/3} n^{2/3}\bar{\gamma}, \quad (3)$$

where n is the number of molecules (in our case NIF molecules) in the nucleus, ϕ is the supersaturation energy parameter, A_i is the surface area of the i-th facet, $\bar{\gamma}$ is the average solid–liquid interfacial energy (contributions from edges and corners are neglected), $\bar{\gamma} = \sum_i A_i\gamma_i / \sum_i A_i$ (γ_i is the solid–liquid interfacial energy of the i-th facet), k is the Boltzmann's constant, T is temperature, S is the supersaturation ratio, k_2 and k_3 are surface and volume shape factors of the nucleus and ν_1 is the volume of a molecule in the solid crystalline phase. The total surface area and the volume of a given nucleus can be expressed in terms of the shape factors and a characteristic dimension, X:

$$\sum_{i=1} A_i = k_2 X^2 \quad (4)$$

$$V' = k_3 X^3. \quad (5)$$

Alternatively, V' can be expressed with the number of molecules constituting the nucleus

$$V' = n\nu_1. \quad (6)$$

The surface area as a function of n (needed for practical application of Eq. (3)) is readily obtained by combining Eqs. (4)–(6).

The number of molecules constituting the critical nucleus $n^{\bullet solution}$ is simply obtained by finding the appropriate extreme of Eq. (3), that is, by differentiating $W^{solution}$ with respect to n and setting the derivative to zero:

$$\frac{\partial W^{solution}}{\partial n} = -kT\ln S + \frac{2\bar{\gamma}}{3}\left(\frac{\nu_1 k_2{}^{3/2}}{k_3}\right)^{2/3} n^{-1/3} = 0 \quad (7)$$

$$n^{\bullet solution} = \frac{8\bar{\gamma}^3(\nu_1 k_2^{3/2}/k_3)^2}{27(kT\ln S)^3}. \quad (8)$$

Since $n\nu_1$ is equal to k_3X^3, the characteristic dimension of the critical nucleus is

$$X^{\bullet solution} = \frac{k_2\nu_1\gamma}{k_3 kT\ln S}, \quad (9)$$

$$W^{\bullet solution} = \frac{8\nu_1^2 k_2^3\bar{\gamma}^3}{27k_3^2(kT\ln S)^2}, \quad (10)$$

where ($^\bullet$) in the superscript denotes a property of the critical nucleus.

Eqs. (8)–(10) can be viewed as general thermodynamic criteria for estimation whether a restricted space is large enough that crystallization of a given substance from saturated solution can occur or not.

2.2. Crystallization from amorphous solid phase in restricted space

If, for some reason (e.g., space restriction as shown above), formation of critical nuclei in supersaturated solution is prevented, then amorphous rather than crystalline solid phase will form upon removal of solvent. The amorphous form, however, is thermodynamically unstable and will eventually crystallize—if the process is not excessively kinetically hindered. In the following, we present the thermodynamical conditions that must be satisfied for the process of crystallization from amorphous phase within a restricted space to occur.

Again we assume that all restricted spatial domains (pores) are of the same shape and size. Let the pores be filled with an amorphous phase. According to the classical nucleation theory, in which strain effects are neglected (Rowlands and James, 1979a,b; Rao and Rao, 1987; Christian, 2002), the free energy of formation of a crystalline nucleus within an amorphous phase, W^a, is given by:

$$W^a = V'\Delta G_V + \sum_i A_i\bar{\gamma}_{ss} \equiv k_3X^3\Delta G_V + k_2X^2\bar{\gamma}_{ss}, \quad (11)$$

where V' is the volume of the nucleus, A_i is the surface area of the i-th facet of the nucleus, is the average interfacial energy between the crystalline and the amorphous phase, $\bar{\gamma} = \sum_i A_i\gamma_i / \sum_i A_i$ (γ_i is the interfacial energy between the crystalline and the amorphous phase of the i-th facet), k_2 and k_3 are shape factors of the nucleus and X is the characteristic dimension of the nucleus. ΔG_V in Eq. (11) represents the decrease in Gibbs free energy when a crystalline nucleus is formed in the amorphous phase (Gibbs free energy of transformation), $\Delta G_V = -(\Delta G/V_m) \equiv -(\Delta G\rho/M)$, where ΔG is the free energy difference between the crystalline and the amorphous state.

The choice of dimension X in Eq. (11) is arbitrary. The characteristic dimension of the critical nucleus is obtained maximization of Eq. (11):

$$X^{\bullet a} = -\frac{2k_2\bar{\gamma}_{ss}}{3k_3\Delta G_V} \quad (12)$$

which, in turn, leads to the activation energy for crystallization:

$$W^{\bullet a} = \frac{4k_2^3\bar{\gamma}_{ss}^3}{27k_3^2\Delta G_V^2}, \tag{13}$$

where ($^\bullet$) in the superscript denotes a property of the critical nucleus. $W^\bullet$ can be regarded as a thermodynamic barrier for the process of crystallization. ΔG can be approximated using Hoffman's equation (Hoffman, 1958):

$$\Delta G = \frac{\Delta H_f \Delta T}{T_m}\left(\frac{T}{T_m}\right), \tag{14}$$

where ΔH_f is the enthalpy of fusion, $\Delta T = T_m - T$ and T_m is the melting point temperature.

γ_{ss} can be approximated using Turnbull's empirical relation: (Turnbull, 1950b)

$$\gamma_{ss} = \frac{C_T \Delta H_{tr}}{(N_A V_m^2)^{1/3}}, \tag{15}$$

where C_T is the Turnbull coefficient (e.g., $C_T = 0.32$ for non-metalic solids), ΔH_{tr} is the enthalpy of the solid–solid transition (crystallization) and V_m is the molar volume of the crystalline phase. This relation cannot be applied generally. For example, it is not entirely appropriate for *n*-alkanes or polymeric systems with enabled free rotation. However, it seems to be a fairly good approximation for certain inorganic compounds (Bartell and Dibble, 1991; Huang and Bartell, 1994; Zhu, 2004; Zhu and Chen, in press) and rigid organic molecules (Huang et al., 1996). Since the molecule considered in the present paper (NIF) is almost entirely rigid, we estimate that Eq. (15) should be applicable. However, there is another deficiency of Eq. (15)—it does not include a temperature dependence of interfacial energy, so it can only be applied within a small interval around the temperature of transition. It should be pointed out that data for amorphous-crystalline interfacial energies involving pharmaceuticals are rarely known. In the case of indometacine, where the experimental values for γ_{ss} are known (Andronis and Zografi, 2000), Eq. (15) gives accurate predictions.

Substituting Eqs. (14) and (15) into Eq. (12), we obtain

$$X^{\bullet a} = \frac{2k_2 C_T T_m^2 M \Delta H_{tr}}{3k_3 (N_A V_m^2)^{1/3} \Delta T T \rho \Delta H_f} \tag{16}$$

and for the number of molecules in the critical nucleus:

$$n^{\bullet a} = \frac{1}{v_1 k_3{}^2}\left(\frac{2k_2 C_T T_m^2 M \Delta H_{tr}}{3(N_A V_m^2)^{1/3}\rho \Delta H_f \Delta T T}\right)^3 \tag{17}$$

Eq. (16) can be used for a first estimation of the dimension of the critical nucleus.

In a more advanced approach to homogenous nucleation in the amorphous phase, $W^\bullet$ is determined taking into account an interplay between three terms: the Gibbs free energy of transformation, the energy required to create an interface between two phases and the strain energy. For many transformations in the solid state, the strain energy is believed to govern the free energy barrier and the shape of the nucleus (Rao and Rao, 1987). It has been shown (Schmelzer et al., 2004; Fokin et al., 2005) that near and below the glass transition temperature, T_g, elastic strains result in thermodynamic inhibition of the crystallization processes. Below T_g the inhibiting term is of the same order of magnitude as, or may even exceed, the thermodynamic driving force for crystallization (Schmelzer et al., 1995).

In order to take into account the influence of elastic stresses on the nucleation process (Fokin et al., 2005), one has to introduce an additional term, G_V^{ed}, into the expression for the work of formation, W^a, of an arbitrary-sized crystalline cluster in the amorphous state:

$$W^a = V'(\Delta G_V + G_V^{ed}) + \sum_i A_i \bar{\gamma}_{ss}$$

$$\equiv k_3 X^3(\Delta G_V + G_V^{ed}) + k_2 X^2 \bar{\gamma}_{ss}, \tag{18}$$

where G_V^{ed} is the energy of elastic deformation connected with the formation of a cluster of volume V', $G_V^{ed} = (G^{ed}/V_m)$. The dimension of the critical nucleus and the activation energy then become:

$$X^{\bullet a} = -\frac{2k_2\bar{\gamma}_{ss}}{3k_3(\Delta G_V + G_V^{ed})} \tag{19}$$

$$W^{\bullet a} = \frac{4k_2^3\bar{\gamma}_{ss}^3}{27k_3^2(\Delta G_V + G_V^{ed})^2} \tag{20}$$

There may exist other effects, such as adsorption of the amorphous form on the pore walls, hydrogen bonding between silica's silanol groups and nifedipine's carbonyl groups, etc., that contribute to stabilization of amorphous NIF. An excellent review of thermodynamic aspects of crystallization in pores was given recently by Scherer (1999). Taking such additional possibilities into account, we may conclude that the critical dimensions and energies derived above present the minimum values for crystallization to occur. In other words, the amorphous state may be stable even within larger spaces than predicted by the present equations.

3. Materials and methods

When exposed to light, nifedipine decomposes to nitroso- and nitro-derivatives (Budvári-Báráni and Szász, 1990). For this reason all procedures were carried out under light protected conditions.

3.1. Preparation of NIF doped xerogels

Xerogels were prepared by acid catalyzed hydrolysis of tetraethyl orthosilicate (TEOS, Merck)

$$(EtO)_4Si + 4H_2O \rightarrow Si(OH)_4 + 4EtOH \tag{21}$$

followed by polycondensation

$$nSi(OH)_4 \rightarrow nSiO_2 + 2nH_2O \tag{22}$$

TEOS, distilled water, ethanol (Riedel de Häen) and citric acid (Aldrich) were used in a molar ratio of 1/7/5/0.1.

Table 1
Synthesis parameters for NIF doped xerogels

Sample/molar ratio	TEOS	Water	Ethanol	Citric acid	NIF
1. Mixing at room temperature					
SNO	1	7	5	0.1	0
SN1	1	7	5	0.1	0.0191
SN2	1	7	5	0.1	0.0229
SN3	1	7	5	0.1	0.0267
SN4	1	7	5	0.1	0.0343
SN5	1	7	5	0.1	0.0381
SN6	1	7	5	0.1	0.0459
SN7	1	7	5	0.1	0.0574
2. Gelation at 60 °C					
3. Drying at 60 °C					

Specifically, for preparation of NIF doped xerogels, TEOS, water, ethanol and citric acid were mixed at room temperature to form a homogenous solution, then NIF (Lek) was added to the solution. The samples were then placed in sealed containers and stored at 60 °C. In this stage, gelation of silica sols took place. After 48 h, the containers were opened and the samples were left to dry for another period of 48 h at 60 °C. In this stage, evaporation of the solute (water and ethanol) took place. After the precipitation of NIF had been completed, transparent yellowish, crack free monoliths were obtained. Table 1 presents the detailed synthesis parameters.

Sample SIN1 was prepared by mixing silica (Riedel de Häen) and NIF at room temperature in a molar ratio 1/0.0191.

Before the experiments were carried out, all samples had been stored at room temperature under light protected conditions for 1 month.

3.2. Specific surface area and porosity parameters

Specific surface area and porosity parameters were determined using the Brunauer–Emmet–Teller (BET) technique based on nitrogen gas adsorption (TRISTAR 3000). Prior to that, the samples were crushed and outgassed.

3.3. Powder X-ray diffraction

To check if any crystalline NIF is present on the surface of the composites X-ray diffraction measurements were carried out with a Siemens D-5000 apparatus using Cu K1 line. The samples were previously crushed.

3.4. Differential thermal analysis (DTA) and thermogravimetric analysis (TGA)

DTA-TGA measurements were performed in Pt–Rh crucibles using a STA 409C/CD apparatus from NETZSCH from room temperature to 900 °C in air conditions with a rate of temperature increase of 10 K/min. Approximately 60 mg of samples were used. The samples were previously crushed. The instrument was calibrated using standard reference materials.

3.5. Differential scanning calorimetry (DSC)

DSC analysis was carried out with a Perkin Elmer Pyris 1 instrument from room temperature to 180 °C in a nitrogen atmosphere (20 ml/min) with a rate of temperature increase of 10 K/min. The samples were previously crushed. The measurements were performed in Al pans using approximately 20 mg of samples. The instrument was calibrated using standard reference materials (In, Zn).

The dissolution profiles are reported elsewhere (Maver et al., 2007).

4. Results and discussion

4.1. Solidification of dissolved nifedipine in nanopores of silica

As shown in the theoretical part ((Eqs. (1) and (2)), crystallization from a saturated solution can begin either on the existing solid surfaces or in bulk solution. The components of surface free energies for the present system (solution of nifedipine in silica pores) are shown in Table 2. Given the variations of reported surface free energy for silica, one gets for $\cos\theta$ in Eq. (1) values from −3.5 to −2.5. The fact that all these values are lower than −1 means that there is no static equilibrium between silica and nifedipine. In other words, the nucleation of NIF in the presence of silica is expected to occur in bulk solution (homogeneous nucleation). This justifies the use of Eqs. (8) and (9) for estimation of critical size of nuclei. In this estimation, we assume that crystalline nuclei have either a spherical or a cubical shape. In our case, the exact evaluations of $n^{\bullet}$ and $r^{\bullet}$ are not possible because the exact value of supersaturation ratio, S, cannot be determined. Namely, due to continuous evaporation/removal of the solvent, S is continuously increasing. We presume that the value of S should lie within the interval $1.5 \leq S \leq 10$. According to literature data (Sugimoto, 2001), higher values of S are unlikely, while lower values will result in a larger value for $n^{\bullet}$,

Table 2
Dispersive and specific components of surface free energies (tensions) [mJ/m^2]

γ_s^d	γ_s^p	γ_s
Silica		
76.0[a]	115.0[a]	191.0
77.7[b]	206.0[b]	283.7
35.6[c]	159.8[c]	195.4
71.3[d]	153.6[d]	224.9
NIF		
23.9[e]	12.9[e]	36.8
γ_l^d	γ_l^p	γ_l
Water		
23.2[e]	48.8[e]	72.0[e]

[a] Biliński, 1994.
[b] Biliński and Chibowski, 1983.
[c] Staszczuk et al., 1985.
[d] Wójcik and Biliński, 1988.
[e] Kerč et al., 1994.

Table 3
Data necessary for calculation of X

$\gamma_{NIF/water} = 20.9$ mN/m[a]
$S = 1.5–10$[b]
$M_{NIF} = 346$ g/mol
N_A–Avogadro's number
$\rho_{NIF} = 1.3578$ g/cm^3[c]
$\nu_1 = M_{NIF}/N_A\ \rho_{NIF} = 0.423$ nm^3
$T = 333$ K

[a] Calculated with Eq. (2).
[b] Chosen as the most probable.
[c] Kerč et al., 1994.

Table 4
Shape factors and calculated properties of critical nuclei

Nucleus type	k_2	k_3	nucleation in supersaturated solution		
Critical			$X^\bullet$ (nm)	$r^\bullet$ (nm)	$N^\bullet$
Spherical	4π	$4\pi/3$	14.2–2.5	14.2–2.5	28497–155
Cubical	6	1	28.4–5.0	24.4–4.3	54152–296
Pore restricted					
Spherical	4π	$4\pi/3$	1.23	1.23	18
Cubical	6	1	1.42	1.23	7

which supports our basic hypothesis even stronger. The data necessary for calculation of $X^\bullet$ are presented in Table 3. Shape factors and calculated properties of critical nuclei are listed in Table 4.

Based on the average pore size obtained by BET, one can estimate the maximum volume of the nucleus that can be formed within the pores. Once ν_1 has been calculated, an estimation of the number of NIF molecules in the nucleus within the pore with given size ($r_{pore} = 1.23$ nm-obtained from BET analysis) is possible. For spherical nucleus one gets $n^{pore} = (4\pi(r_{pore})^3/3\nu_1) = 18$ while for cubical nucleus one finds: $n^{pore} = (8(r^{pore})^3/3\sqrt{3}\nu_1) = 7$ (*c.f.* Fig. 2).

These calculations show that formation of a continuous crystalline phase during the solid phase formation cannot occur because the critical nucleus size exceeds the pore size. For example, as shown in Table 4, the critical nucleus consists of 28497-155 NIF molecules (assuming spherical nuclei) or 54152-296 NIF molecules (assuming cubical nuclei). On the other hand, the present pore size only permits accommodation of 18 NIF molecules (if spherical nucleus is assumed) or 7 NIF molecules (for cubical nucleus). Formation of solid phase can thus occur either through formation of discrete subcritical particles or through a continuous increase of concentration up to the point where the molecular mobility is insufficient for crystallization. In the first case, the structural order occurs within a very short range (e.g., up to about 2.5 nm across the pore-restricted nucleus or, in other words, across 3–4 NIF molecules). Conventionally, such materials are regarded amorphous because short ordering cannot be detected using most techniques. In the second case, crystallization is also hindered kinetically. Namely, the concentration of solution can increase to the point where the intermolecular distances are so small that the matter resembles an undercooled melt mixed with the residual solvent.

X-ray diffraction (Fig. 3). XRD patterns of samples SN1-SN6 show no sharp peaks, which means that no crystalline NIF is present on the surface. It must be stressed that XRD is not suitable for detection of phase crystallinity inside the pores, because under such circumstances the Bragg's law cannot be fulfilled. In other words, even if the molecules in the confined particles were perfectly ordered (perfect single crystals) the diffraction patterns would show amorphous behaviour. By contrast, sample SN7 does show small peaks at angles that correspond to the peaks of crystalline NIF. It is assumed that this NIF-rich

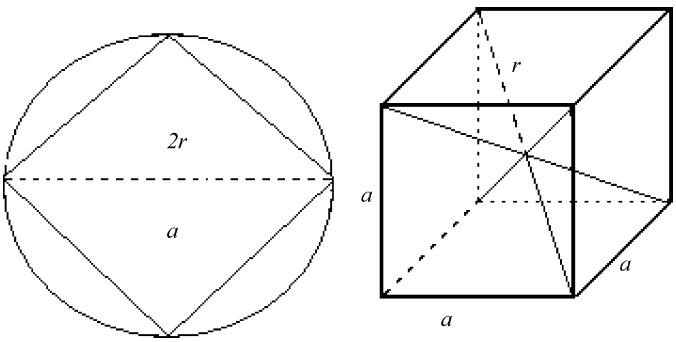

Fig. 2. Transverse section of a cubical nucleus in a pore. Graphical representation of geometrical parameters used in derivation of the critical dimensions of nuclei.

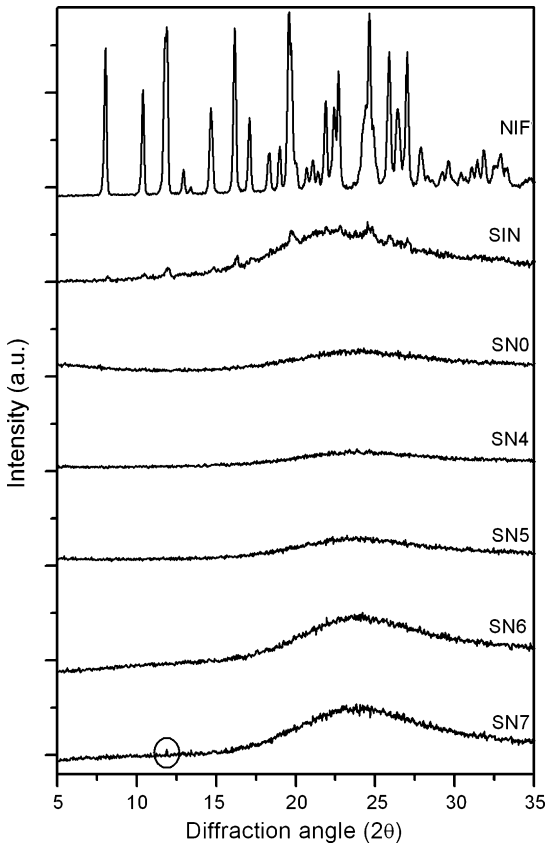

Fig. 3. X-ray powder diffraction patterns of crystalline NIF, SIN, SN0, SN4, SN5, SN6 and SN7. At the present resolution, the patterns of samples SN1, SN2, SN3 are indistinguishable from the pattern of sample SN0 and, hence, are not shown.

sample contains more NIF than can be accommodated within the pores of silica. It is reasonable to expect that the surplus of NIF that is accommodated outside the pores will have enough space to crystallize. To check the consistency of these results, we also measured the X-ray of a simple physical mixture of NIF and silica (sample SIN) having the same nominal composition as sample SN1. As expected, it was found that NIF, when physically mixed with silica, had a well-defined crystalline nature.

The method of choice for identification of crystallinity of typical organic substances, such as drugs, is DSC. For example, the DSC curve of crystalline NIF exhibits an endothermic peak at 172 °C with an enthalpy change of 108.19 J/g (37433 J/mol), which is due to melting of form A (Hirayama et al., 1994). In the case of amorphous NIF (prepared by quenching), however, an exothermic peak arises between 100 and 120 °C with an enthalpy change of −52.95 J/g (−18320 J/mol), which is due to crystallization into form A (Hirayama et al., 1994). After that an endothermic peak is again seen at 172 °C, due to melting of form A.

Because of the finite-size effect, a shift in the melting temperature of confined NIF is expected according to the Gibbs–Thomson equation, but a melting peak will still be observed.

DSC curves of all NIF doped xerogels exhibit a broad endothermic rise between 60 and 160 °C. This agrees with the obtained DTA and TGA data (DTA-TGA curves of samples SN0 and SN7 are shown in Fig. 4) where all the samples exhibit an endothermic peak and a weight loss due to the evaporation of the remaining water and ethanol (Yang et al., 1999; Brinker and Scherer, 1990). The DSC curves of crystalline and amorphous NIF, SN4 and SN7 are presented in Fig. 6a. In the case of samples SN1, SN2, SN3 and SN4 no melting peak is observed which confirms that NIF is present in the amorphous form (Fig. 5a). In the case of sample SIN1 (Fig. 5a), a physical mixture of NIF and silica with the same fraction of NIF as that in SN1 (the sample with lowest NIF load), a clearly defined melting peak is observed at 172 °C, which demonstrates that the smallest load is detectable with DSC. The curves of samples SN5 and SN6 show a small melting peak at 172 °C with enthalpy changes of 1.47 and 2.42 J/g, respectively (Fig. 5b). In the case of sample SN7 (Fig. 5a) the melting peak is even more pronounced ($\Delta H_f = 21.00$ J/g). An endothermic peak due to melting is also observed in the curve of sample SN4 which was previously milled (SN4 milled) (Fig. 5b). Those peaks indicate that

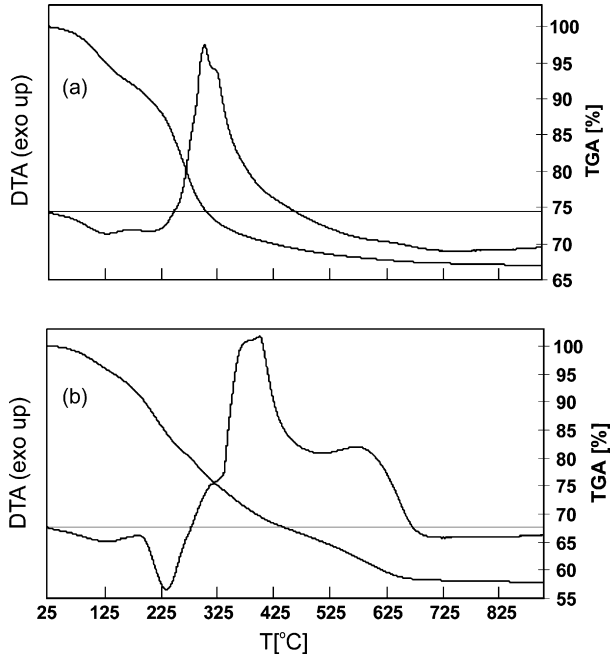

Fig. 4. DTA and the corresponding TGA curves of samples (a) SN0 and (b) SN7.

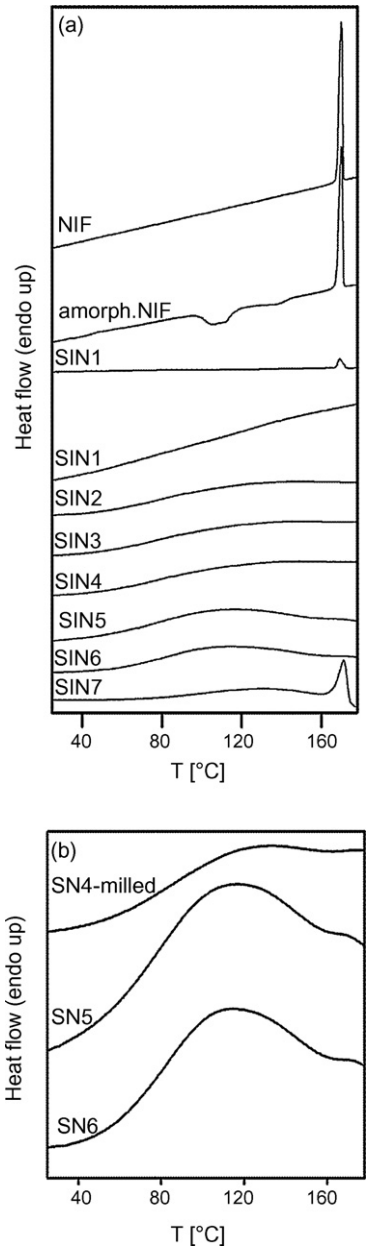

Fig. 5. DSC thermograms of samples (a) crystalline NIF, amorphous NIF and samples SN1–7. (b) Magnified DSC curves for samples SN4 milled, SN5, and SN6 that show traces of melting peak at 172 °C.

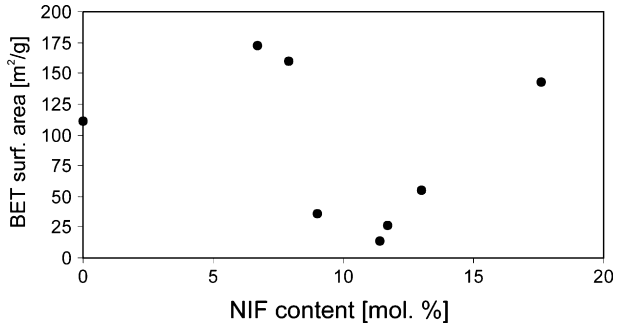

Fig. 6. Variation of specific surface area as a function of the total amount of NIF in the prepared samples.

a small amount of crystalline NIF is present in these samples. The fact that there is no shift in melting temperature confirms the existence of macroscopic crystalline NIF particles, which are not accommodated in the pores.

To understand better the transition from complete amorphicity in samples with low NIF content to increasing crystallinity at higher NIF contents, we measured the corresponding variation of specific surface area (Fig. 6). Addition of small amounts of NIF to porous silica increases the total surface area—due to the additional surface area of added NIF. With increasing content of NIF the pores get more and more filled and the total surface area decreases to the point where the pores are full (see schematics in Fig. 7). Based on the results of Fig. 6, we suppose that this happens in sample SN4 containing 11.4% of NIF where the surface area has the smallest value. Because in sample SN4 (and all samples containing less NIF) all nifedipine is entrapped within the porous system, it is theoretically expected that samples SN1-4 will not exhibit any crystallinity. The results of DSC are in complete agreement with this prediction. XRD shows crystallinity only in sample SN7; probably this technique is less sensitive in the present case. Upon further addition of NIF, the surface area increases again (see Fig. 6). We assume that now NIF is being deposited on the surface of silica particles or between the particles (see schematics in Fig. 7). In either case, there is much more space for nucleation and crystallization of NIF. This explains why in samples SN5-7 increasing amounts of crystalline NIF are observed.

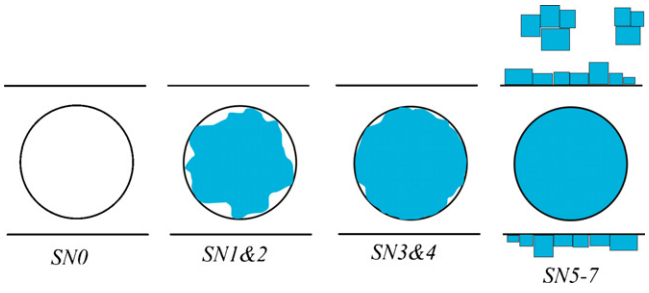

Fig. 7. Schematic representation of deposition of amorphous NIF (blue area) inside silica pores and formation of NIF crystallites on outer silica surfaces and/or between silica particles.

Table 5
Data necessary for the calculation of $X^{\bullet}$ [a]

$\Delta H_f = 37433.74$ J/mol[a]
Absolute value of $\Delta H_{tr} = 18320.70$ J/mol[b]
$M_{NIF} = 346$ g/mol
N_A–Avogadro's number
$\rho_{NIF} = 1.358$ g/cm^3[c]
$\nu_1 = M_{NIF}/N_A\ \rho_{NIF} = 0.423$ nm^3
$V_m = 254.8$ cm^3/mol
$T_g = 321$ K[d]

[a] From DSC analysis.
[b] From DSC analysis.
[c] Kerč et al., 1994.
[d] Keymolen et al., 2003.

4.2. Stability of amorphous nifedipine within the silica pores

As shown in the theoretical part, the amorphous state of matter is inherently unstable and has a tendency to transform into crystalline state. However, as further pointed out, this transformation can be inhibited—if the matter is confined into small enough spaces. The data necessary for calculation of $X^{\bullet}$ [a] are presented in Table 5. The dimension of the critical nucleus was calculated for the temperature interval between $T_m/2$ and T_m. The calculated temperature dependence of the dimension of the critical nucleus is shown in Fig. 8. Below T_g, G_V^{ed} is assumed to be constant ($G_V^{ed} = 107\,J/m^3$). Above T_g the dotted lines represent $X^{critical}$ in absence of elastic strain effects and the curved ones are calculated for the case when elastic strains are taken into account. The upper curve represents the calculation for the cubical nucleus and the lower for the spherical nucleus. For both shapes studied (spherical, cubical) and at all temperatures the values of calculated critical parameters are larger than the experimentally observed values in the present porous systems, so transition from amorphous to crystalline NIF is theoretically not expected.

The theoretical calculation is fully consistent with the results of DSC where no crystallization peaks in doped xerogels SN1–SN4 could be observed. In other words, in these xerogels the amorphous form is stable at least up to the melting

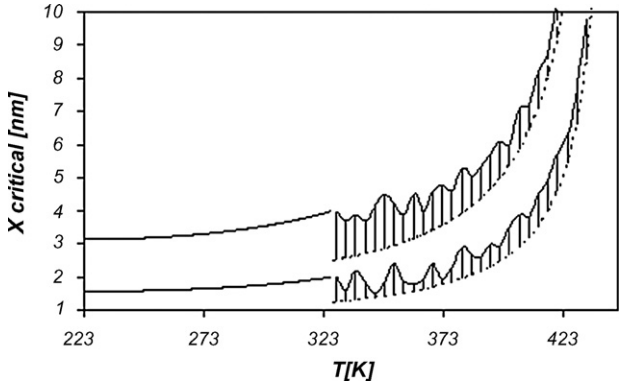

Fig. 8. Calculated temperature dependence of $X^{\bullet}$ between $T_m/2$ and T_m. The hatched curve indicates that the exact upper limit is not known due to uncertainty of elastic strain data.

point. In fact, DTA analysis showed that the samples were thermally stable even up to about 260 °C where the combustion of organic compounds began (appearance of exothermic region). Consistently, the area of the exothermic region increased with increasing amount of NIF. However, if for example, sample SN4 was first milled and only then thermally treated, a melting peak was clearly observed (Fig. 5b). It is supposed that milling breaks the silica network thus releasing a significant amount of amorphous NIF originally entrapped in silica pores. Consistently with the present theoretical interpretation, the amorphous NIF is expected to crystallize—once out of nanosized pores. The same effect, although at a lesser extent, was observed in crushed samples.

5. Conclusions

Incorporation of NIF into a silica xerogel with an average pore diameter of about 2.5 nm produces and stabilizes its amorphous form. The confined amorphous NIF is effectively protected against crystallization within the temperature range in which NIF itself is stable. Namely, the entrapment of a drug inside nanosized pores prevents thermodynamically the formation of critical nuclei needed for crystallization. If the matrix of the carrier breaks, there is no more space restriction and the drug will crystallize. We have shown by a generalized treatment that the total amount of a drug that can be stabilized in the amorphous state depends on the total pore volume of the given xerogel and on the extent of stress introduced (for example by crushing or milling). Since, in principle, no specific interactions are necessary, the method could be considered as a general approach to stabilization of amorphous substances. If the pore size of the carrier satisfies the conditions $r_{\text{pore}} < -(k_2 \nu_1 \gamma / k_3 kT \ln S)$ and $r^{\text{pore}} < -(2k_2 \bar{\gamma}_{\text{ss}} / 3k_3(\Delta G_{\text{V}} + G_{\text{V}}^{\text{ed}}))$, the method produces a stable amorphous form, providing that the contact angle between the embryo and the carrier surface is higher than π. If these conditions are not fulfilled, the critical nucleus size is lowered due to the presence of a catalytic surface. Then an amorphous phase can still form (if only the first inequality holds), but it will be unstable and will eventually crystallize. Alternatively (if none of the conditions is satisfied), a crystalline phase will preferentially form. These conditions should be interpreted with sufficient care because they do not take into account the kinetics of solidification. Additionally, it is necessary to stress that in our treatment we use macroscopic rather than "nanoscopic" values of physical-chemical properties. Although the use of macroscopic properties in the classical nucleation theory is justified in most cases, we have no evidence that this is also so in our particular case. Nevertheless, the present treatment shows clearly that in small enough confined spaces (such as nanosized pores) the observed state of a solid will be the amorphous rather than the crystalline state.

Acknowledgments

Financial support from The Ministry of Higher Education, Science and Technology of the Republic of Slovenia, the National Institute of Chemistry and the Faculty of Pharmacy is gratefully acknowledged.

References

Adamson, A.W., Gast, A.P., 1997. Physical Chemistry of Surfaces, 6th ed. John Wiley & Sons Inc., USA, pp. 329–332.

Ahola, M., Kortesuo, P., 2000. Silica xerogel carrier material for controlled release of toremifene citrate. Int. J. Pharm. 195, 219–227.

Andronis, V., Zografi, G., 2000. Crystal nucleation and growth of indomethacin polymorphs from the amophous state. J. Non-Cryst. Solids 271, 236–248.

Bartell, L.S., Dibble, T.S., 1991. Electron diffraction studies of the kinetics of phase changes in molecular clusters. Freezing of CCl_4 in supersonic flow. J. Phys. Chem. 95, 1159–1167.

Biliński, B., Chibowski, E., 1983. The determination of the dispersion and polar free surface energy of quartz by the elution gas chromatography method. Powder Technol. 35, 39.

Biliński, B., 1994. The influence of surface dehydroxylation and rehydroxylation on the components of surface free energy of silica gels. Powder Technol. 81, 241.

Bögershausen, A., Pas, S.J., Hill, A.J., Koller, H., 2007. Drug release from self-assembled inorganic-organic hybrid gels and gated porosity detected by positron annihilation lifetime spectroscopy. Chem. Mater. 18, 664–672.

Böhlmann, W., Pöppl, A., Michel, D., 1999. Electron spin resonance studies of copper complexes incorporated in zeolites and mesoporous molecular sieves. Colloids Surf. A: Physicochem. Eng. Aspects 158, 235–240.

Brinker, C.J., Scherer, G.W., 1990. Sol–Gel Science: The Physics and Chemistry of Sol–Gel Processing. Academic press, New York, pp. 547–615.

Budvári-Báráni, Z., Szász, G., 1990. Some new data concerning the chromatographic purity test for nifedipine. J. Liq. Chromatogr. 13, 3541–3551.

Chen, X., Dong, S., 2003. Sol–gel-derived titanium oxide/copolymer composite based glucose biosensor. Biosens. Bioelectron 18, 999–1004.

Chong, A.S.M., Zhao, X.S., 2004. Functionalized nanoporous silicas for the immobilization of penicillin acylase. Appl. Surf. Sci. 237, 398–404.

Christian, J.W., 2002. The Theory of Transformations in Metals and Alloys. Elsevier Science Ltd., Oxford UK, pp. 422–479.

Chytil, S., Glomm, W.R., Wollebekk, E., Bergen, H., Walmsley, J., Sjöblom, J., Blekkan, E.A., 2005. Platinum nanoparticles encapsulated in mesoporous silica: Preparation, characterisation and catalytic activity in toluene hydrogenation. Microporous and Mesoporous Mater. 86, 198–206.

Czuryszkiewicz, T., Ahvenlammi, J., Kortesuo, P., Ahola, M., Kleitz, F., Jokinen, M., Linden, M., Rosenholm, J.B., 2002. Drug release from biodegradable silica fibers. J. Non-Cryst. Solids 306, 1–10.

Defay, R., 1966. Surface Tension and Adsorption. Longmans, Green & Co. Ltd., London, p. 310.

Fokin, V.M., Zanotto, E.D., Schmelzer, J.W.P., 2005. New insights on the thermodynamic barrier for nucleation in glasses: The case of lithium disilicate. J. Non-Cryst. Solids 351, 1491–1499.

Hirayama, F., Wang, Z., Uekama, K., 1994. Effect of 2-hydroxypropyl-beta-cyclodextrin on crystallization and polymorphic transition of nifedipine in solid-state. Pharm. Res. 11, 1766.

Hoffman, J.D., 1958. Thermodynamic drivig force in nucleaion and growth processes. J. Chem Phys. 29, 1192.

Huang, J., Bartell, L.S., 1994. Electron diffraction studies of the kinetics of phase changes in clusters. 4. Freezing of ammonia. J. Phys. Chem. 98, 4543–4550.

Huang, J., Lu, W., Bartell, L.S., 1996. Isomeric differences in the nucleation of crystalline hydrocarbons from their melts. J. Phys. Chem. 100, 14276–14280.

Jackson, C.L., McKenna, G.B., 1996. Vitrification and crystallization of organic liquids confined to nanoscale pores. Chem. Mater. 8, 2128–2137.

Kerč, J., Srčič, S., Planinšek, O., Kofler, B., 1994. Contact angles and surface free energy parameters of some 1,4-dihydropyridine calcium antagonist powders. Farm. Vestn. 45, 347–357.

Keymolen, B., Ford, J.L., Powell, M.W., Rajabi-Siahboomi, A.R., 2003. Investigation of the polymorphic transformations from glassy nifedipine. Thermochim. Acta 397, 103–117.

Kim, J.K., Park, J.K., Kim, H.K., 2004. Synthesis and characterization of nanoporous silica support for enzyme immobilization. Colloids Surf. A: Physicochem. Eng. Aspects 241, 113–117.

Kim, J., Jia, H., Lee, C., 2006. Single enzyme nanoparticles in nanoporous silica: A hierarchical approach to enzyme stabilization and immobilization. Enzyme Microb. Technol. 39, 474–480.

Kortesuo, P., Ahola, M., 2001. In vitro release of dexmedetomidine from silica xerogel monoliths: effect of sol–gel synthesis parameters. Int. J. Pharm. 221, 107–114.

Kortesuo, P., Ahola, M., 2002. Effect of synthesis parameters of the sol–gel-processed spray-dried silica gel microparticles on the release rate of dexmedetomidine. Biomaterials 23, 2795–2801.

Lucas, A., Gaudé, J., Carel, C., Michel, J.-F., Cathelineau, G., 2001. A synthetic aragonite-based ceramic as a bone graft substitute and substrate for antibiotics. Int. J. Inorg. Mater. 3, 87–94.

Maria Chong, A.S., Zhao, X.S., 2004. Design of large-pore mesoporous materials for immobilization of penicillin G acylase biocatalyst. Catal. Today 93–95, 293–299.

Maver, U., Godec, A., Bele, M., Planinšek, O., Gaberšček, M., Jamnik, J., 2007. Novel hybrid silica xerogels for stabilization and conrtolled release of drug. Int. J. Pharm. 330, 164–174.

Möller, J., Schmelzer, J., Gutzow, I., 1998. Elastic stress effects on critical cluster shapes. J. Non-Cryst. Solids 240, 131–143.

Prasad, S., Quijano, J., 2006. Development of nanostructured biomedical microdrug testing device based on in situ cellular activity monitoring. Biosens. Bioelectron. 21, 1219–1229.

Quaranta, A., Carturan, S., Maggioni, G., Ceccato, R., Della Mea, G., 2003. Probing the chemical environment of 3-hydroxyflavone doped ormosils by a spectroscopic study of excited state intramolecular proton transfer. J. Non-Cryst. Solids 322, 1–6.

Rao, C.N.R., Rao, K.J., 1987. Phase Transformations in Solids. McGraw-Hill, New York.

Rowlands, E.G., James, P.F., 1979a. Analysis of steady state crystal nucleation rates in glasses. Part 1. Methods of analysis and application to lithium disilicate glass. Phys. Chem. Glasses 20, 1–8.

Rowlands, E.G., James, P.F., 1979b. Analysis of steady state crystal nucleation rates in glasses. Part 2. Further comparison between theory and experment for lithium disilicate glass. Phys. Chem. Glasses 20, 9–14.

Scherer, G.W., 1999. Crystallization in pores. Cement Concrete Res. 29, 1347.

Schmelzer, J., Möller, J., Gutzow, I., 1995. Surface energy and structure effects on surface crystallization. J. Non-Cryst. Solids 183, 215–233.

Schmelzer, J.W.P., Potapov, O.V., Fokin, V.M., Müller, R., Reinsch, S., 2004. The effect of elastic stress and relaxation on crystal nucleation in lithium disilicate glass. J. Non-Cryst. Solids 333, 150–160.

Shankaran, D.R., Uehara, N., Kato, T., 2003. A metal dispersed sol–gel biocomposite amperometric glucose biosensor. Biosens. Bioelectron. 18, 721–728.

Shin, Y., Chang, J.H., 2001. Hybrid nanogels for sustainable positive thermosensitive drug release. J. Controlled release 73, 1–6.

Shneidman, A., Weinberg, M.C., 1996. Crystallization of rapidly heated amorphous solids. J. Non-Cryst. Solids 194, 145–154.

Slezov, V.V., Schmelzer, J., Tkach, Ya.Y., 1997. Nucleation of a one-component new phase in a solid solution under different conditions. J. Phys. Chem. Solids 58, 869–880.

Sliwinska-Bartkowiak, M., Dudziak, G., Grass, R., 2001. Freezing behavior in porous glasses and MCM-41. Colloids Surf. A: Physicochem. Engin. Aspects 187/188, 523–529.

Sotiropoulou, S., Vamvakaki, V., 2005. Stabilization of enzymes in nanoporous materials for biosensor applications. Biosens. Bioelectron. 20, 1674–1679.

Staszczuk, P., Jańczuk, B., Chibowski, E., 1985. On the determination of the surface free energy of quartz. Mater. Chem. Phys. 12, 469.

Sugimoto, T., 2001. Monodispersed particles. Elsevier Science B.V., The Netherlands.

Tian, D., Blacher, S., 1999. Biodegradable and biocompatible inorganic–organic hybrid materials. 4. Effect of acid content and water content on the incorporation of aliphatic polyesters into silica by the sol–gel process. Polymer 40, 951–957.

Turnbull, D., 1950a. Kinetics of heterogeneous nucleation. J. Chem. Phys. 18, 198–203.

Turnbull, D., 1950b. Formation of crystal nuclei in liquid metals. J. Appl. Phys. 21, 1022–1028.

Vallet-Regi, M., Doadrio, J.C., Doadrio, A.L., Izquierdo-Barba, I., Pérez-Pariente, J., 2004. Hexagonal ordered mesoporous material as a matrix for the controlled release of amoxicillin. Solid State Ionics 172, 435–439.

Volmer, M., 1929. Über Keimbildung und Keimwirkung als Spezialfiille der heterogenen Katalyse. Z. Elektrochem. 35, 555.

Volmer, M., 1939. Kinetik der Phasenbildung. Steinkopf, Dresden.

Wakayama, Y., Tagami, T., Tanaka, S., 1999. Three-dimensional islands of Si and Ce formed on SiO_2 through crystallization and agglomeration from amorphous thin films. Thin Solid Films 350, 300–307.

Wang, W., Song, M., 2006. Multistep impregnation method for incorporation of high amount of titania into SBA-15. Mater. Res. Bull. 41, 436–447.

Wójcik, W., Biliński, B., 1988. Gas-adsorption studies on correlations between the flotability of minerals and the work of water adhesion to their surfaces. Colloids Surf. 30, 275.

Wu, S., 1971. Calculation of interfacial tensions in polymer sysrems. J. Polymer. Sci. Part C 34, 19–30.

Yang, H.S., Choi, S.Y., Hyun, S.H., Park, C.G., 1999. Ambient-dried SiO_2 aerogel thin films and their dielectric application. Thin Solid Films 348, 69.

Zhao, L., Zhu, G., Zhang, D., Chen, Y., Qiu, S., 2005. A surface modification scheme for incorporation of nanocrystals in mesoporous silica matrix. J. Solid State Chem. 187, 2980–2986.

Zhu, X., 2004. Molecular dynamics study of homogeneous nucleation in supercooled clusters of sodium bromide. J. Mol. Struct. (Theochem) 680, 137–141.

Zhu, X., Chen, K., in press. Molecular dynamics simulation of homogeneous nucleation of KBr cluster. J. Phys. Chem. Solids, 1–7.

Zusman, R., Rottman, C., Ottolenghi, M., Avnir, D., 1990. Doped sol–gel glasses as chemical sensors. J. Non-Cryst. Solids 122, 107–109.